Science of The Total Environment, Volume 712, April 2020, Article number 136413
DOI:10.1016/j.scitotenv.2019.136413

Disinfection by-product formation during UV/Chlorine treatment of pesticides in a novel UV-LED reactor at 285 nm and the mitigation impact of GAC treatment

Irene Carra[1*], Javier Fernandez Lozano[1], Olivier Autin[2], James R. Bolton[3], Peter Jarvis[1]

[1]Cranfield University, College Rd, Cranfield, MK430AL, UK

[2]Typhon Treatment Systems, Penrith, CA110BT, UK

[3]Bolton Photosciences Inc., 628 Cheriton Cres., NW, Edmonton, AB T6R 2M5, Canada

[*]corresponding Author: Irene.carra@cranfield.ac.uk; Cranfield University, College Rd, Cranfield, MK430AL, UK

Abstract

The UV/Chlorine process has gained attention in recent years due to the high quantum yield and absorbance of the chlorine species. However, there are still many unknowns around its application as a treatment for drinking water. The potential for the formation of disinfection by-products (DBPs) is one of them. There are no studies reporting on the formation of Trihalomethanes (THMs) or Haloacetic Acids (HAAs) in complex matrices, such as real source waters, at UV wavelengths tailored to the UV/Chlorine process, which has been possible thanks to the development of Light Emitting Diodes (LEDs). In addition, consideration of mitigation measures that might be needed after UV/chlorine treatment for full scale application have not been previously reported. Specifically, the novelty of this work resides in the use of an innovative reactor using UV-LEDs emitting at 285 nm for the removal of three pesticides (metaldehyde, carbetamide and mecoprop), the evaluation of THM, HAA and bromate formation in real water

Published by Elsevier. This is the Author Accepted Manuscript issued with: Creative Commons Attribution Non-Commercial No Derivatives License (CC:BY:NC:ND 4.0). The final published version (version of record) is available online at DOI:10.1016/j.scitotenv.2019.136413. Please refer to any applicable publisher terms of use.

sources by UV/Chlorine treatment and the mitigation effect of subsequent GAC treatment. A new parameter, the Applied Optical Dose (AOD), has been defined for UV reactors, such as the one in the present study, where the irradiated volume is non-uniform. The results showed the feasibility of using the UV/Chlorine process with LEDs, although a compromise is needed between pH and chlorine concentration to remove pesticides while minimising DBP formation. Overall, the UV/Chlorine process did not significantly increase THM or HAA formation at pH 7.9-8.2 at the studied wavelength. At acidic pH, however, THM formation potential increased up to 30% after UV/Chlorine treatment with concentrations up to 60 μg/L. HAA formation potential increased between 100-180%, although concentrations never exceeded 35 μg/L. In all cases, GAC treatment mitigated DBP formation, reducing THM formation potential to concentrations between 3-16 μg/L, and HAA formation potential between 4-30 μg/L.

Keywords: Light Emitting Diodes (LEDs); Trihalomethanes (THM); Haloacetic Acids (HAA); bromate; Chlorine; Advanced Oxidation Process (AOP); Activated Carbon; Drinking Water

1 INTRODUCTION

Advanced oxidation processes (AOPs) have been widely reported in the literature as effective treatments to remove persistent micropollutants from water (Miklos et al., 2018; Oturan and Aaron, 2014). The most common AOP used at large scale in water treatment works (WTWs) is UV/H_2O_2, typically run with low or medium pressure lamps. However, UV-AOPs are often associated with high operating costs, as the UV doses required for micropollutants degradation are at least 10 times higher than those used for UV disinfection (Collins and Bolton, 2016).

UV light emitting diodes (LEDs) first emerged at the beginning of the 21st century as an exciting technology offering significant opportunities for AOPs applications and water treatment. LEDs allow for more flexibility towards reactor configuration and predicted low costs (Taghipour and Oguma, 2019). An advantage of LEDs is that they can be developed to emit light over a range of specific wavelengths, such that different pollutants, micro-organisms and oxidants can be targeted. However, it should be born in mind that the available photonic output decreases at lower wavelengths, particularly moving towards the UVC spectral range (200-280 nm) (Beck, 2018). This directly affects AOPs such as UV/H_2O_2 or UV/Persulphate, where the absorption spectrum of the oxidants increases toward shorter wavelengths in the UVC spectral range, and thus LED-based application will need to wait until LEDs in the UVC spectrum further develop.

The UV/Chlorine process has gained attention in recent years. It is often compared to the UV/H_2O_2 process because of its high quantum yield and higher absorbance (Goldstein et al., 2007; Remucal and Manley, 2016). Studies show better performance than the UV/H_2O_2 process under mildly acidic conditions for the removal of some micropollutants (Yang et al., 2016), with the additional advantage that it can be operated at higher wavelengths than the UV/H_2O_2 process. However, it is a complex process, not yet fully understood, partly arising from the fact that aqueous chlorine species are pH dependent and have different light absorption properties (Jin et al., 2011). Nevertheless, the use of chlorine presents certain advantages to hydrogen peroxide. It is a commonly used chemical for disinfection in drinking water treatment, and it is considered safe in its hypochlorite form. Furthermore, it can be economically more viable than the UV/H_2O_2 process because of its lower cost, the potential for lower concentrations required and, thus, the reduction in storage space (Wang et al., 2019).

There are still many unknowns around the application of the UV/Chlorine process as treatment for drinking water. For example, the potential for the formation of disinfection by-products (DBPs) from the reaction between chlorine[1] and organic matter. Some research has been published on the formation of trihalomethanes (THMs) or haloacetic ~~A~~acids (HAAs) after UV/Chlorine treatment with low and medium pressure lamps (Reckhow et al., 2010; Wang et al., 2015; Yang et al., 2016; Zhang et al., 2015; Zhou et al., 2016) . However, there is only one study

[1] Here and elsewhere, when we state “chlorine”, we mean “active” or “free” chlorine.

reporting on THM or HAA formation for synthetic water at tailored wavelengths more specific to the UV/Chlorine process such as 285 nm, which is close to one of the maximum absorption peaks for chlorine (292 nm) (Gao et al., 2019). They reported the increased formation of THMs and HAAs ~~by~~ after UV/Chlorine treatment at 254, 275 and 310 nm. However, this study was carried out in a controlled system with humic acids in ultrapure water using a semi-collimated beam apparatus. However, different organic compounds and the presence of alkalinity and other ions can affect the efficiency of the UV/Chlorine process. The wavelength may not only have an impact on the efficiency of an AOP, but also on the organic by-products formed during treatment. These organic by-products have the potential to form other DBPs. Thus, the wavelength used may have an impact on the type and concentration of DBPs formed. Therefore, further research is needed to understand the impact of the UV/Chlorine process on DBPs at wavelengths specific to this process in more complex water matrices. In the case of inorganic DBPs, the formation of bromate when using the UV/Chlorine process in bromide-rich waters with low, and the use of medium pressure lamps has also been reported, identifying a possible risk of the process through formation of bromate (De Laat and Stefan, 2018; Fang et al., 2017a), outlining the need of further research on this topic. In addition, wider considerations for large scale application of the UV/Chlorine process have yet to be answered. In particular, GAC treatment after oxidation processes is common practice in the UK, but the benefit of GAC adsorption after the UV/Chlorine process to help control DBPs is still unknown.

The aim of this research was therefore to determine the effectiveness of the UV/Chlorine process for the degradation of pesticides in real source waters whilst also considering the wider water quality impact of the process. The novelty of this work resides in the use of a novel bench-scale UV-LED reactor emitting at 285 nm for the removal of three pesticides (metaldehyde, carbetamide and mecoprop), which have been widely reported in water bodies in the UK at concentrations of ng/L (DWI, 2017). For the first time the impact of the UV/Chlorine process on DBP formation (THMs, HAAs and bromate) at 285 nm in real source waters is reported as well as the impact of having GAC treatment after the UV/Chlorine process.

2 MATERIALS AND METHODS

2.1 Chemicals

Metaldehyde (99+% purity) was obtained from Acros. Carbetamide and mecoprop (99+% purity) were obtained from Sigma Aldrich. Purelab Option-S7/15 system (Elga process water, Buckinghamshire, UK) supplied the ultra-pure water.

Sodium hypochlorite (NaClO) 13%, and methanol (HPLC grade) and ammonium formate (99+% purity) used for the mobile phases were provided by Fisher Scientific. Samples were quenched using sodium thiosulfate ($Na_2S_2O_3$, 99% purity) also provided by Fisher Scientific. For THM determination, potassium dihydrogenphosphate (KH_2PO_4) and disodium hydrogenphosphate (Na_2HPO_4)

were obtained from Acros. Sodium sulphite (Na_2SO_3, 99+% purity) and sodium sulphate (Na_2SO_4, 99+% purity) were provided by Fisher Scientific. 1,2,3 trichloropropane, 1,4 bromofluorobenzene, THM calibration mix (EPA 501/601 chloroform, bromodichloromethane chlorodibromomethane and bromoform, compound at 2.0 mg/mL in methanol), HAA calibration mix (EPA 552.2 monochloroacetic acid, dichloroacetic acid, trichloroacetic acid, chlorobromo acetic acid, dichlorobromo acetic acid, chlorodibromo acetic acid, monobromo acetic acid, dibromo acetic acid and tribromo acetic acid each compound at 2.0 mg/mL concentration in methyl tert-butyl ether) and methyl tert-butyl ether (HPLC grade) were obtained from Sigma Aldrich. Sulfuric acid (H_2SO_4) and sodium hydroxide (NaOH, laboratory grade) were obtained from Acros.

2.2 Physicochemical water properties

The experimental work was undertaken using water samples from three different WTWs in the UK. Water samples were taken from a point in the process where an AOP would typically be applied, usually after clarification and rapid gravity filtration or ultrafiltration. WTW A abstracts water directly from a river catchment; WTW B abstracts water from a canal with a blend from three rivers; and WTW C abstracts water from a large surface water reservoir. Samples from WTW A have been called “source A” and were taken after ultrafiltration (UF) membrane treatment, which is preceded by roughing granular activated carbon (GAC) treatment. Samples from WTWs B and C have been called “sources B and C” and were taken after rapid gravity filter treatment, which is preceded by pre-ozonation and clarification (there is no UF or other membrane treatment in these

WTWs). The physicochemical properties of the three sources are shown in Table 1.

Table 1. Physicochemical properties of sources A, B and C.

Parameters	Source A	Source B	Source C
pH	7.9	8.0	8.2
Alkalinity (mg/L as $CaCO_3$)	145	202	174
Chloride (mg/L)	85	82	95
DOC* (mg/L)	2.4	5.2	5.5
Bromate (μg/L)	< 0.35	< 0.35	0.90
Bromide (μg/L)	215	114	153
UVT_{254}** (%)	92	79	87

*Disolved Organic Carbon
**Ultraviolet Transmittance at 254nm

2.3 UV/Chlorine experimental procedure

The experiments were carried out in an innovative single-wavelength LED reactor patented by Typhon Treatment Systems (Macnulty, 2019). The reactor consisted of a 30 mm internal diameter quartz cylinder with two rings of 20 LEDs (one ring on top of the other) (Figure 1). In contrast to other bench scale systems such as collimated beam apparatus or annular reactors, the LED arrays are set around the reactor, not on top or in the centre (Figure 1), resulting in a radial UV distribution with the UV beams focused into the centre. This design is based on Typhon Treatment Systems patented system and differs from conventional bench scale designs such as collimated beam devices where the LEDs or lamps are placed on top of the reactor, or annular reactors where the lamps are placed in

the centre of the reactor. Each LED has a photonic output of 100 mW emitting at 285 nm, and a total reactor volume of 3.15 L. The use of 285 nm was selected because it is close to the maximum absorption peak of the hypochlorite ion, but so far no studies report on its impact on DBP formation potential after UV/Chlorine treatment. To prevent the LED chips from overheating, the reactor included a cooling system. The irradiation time was controlled through software linked to the LED performance. This reactor has the same light diffusion properties as the full scale configuration, including identical reactor material and diameter, LEDs and disposition, enabling laboratory and full scale results to be.

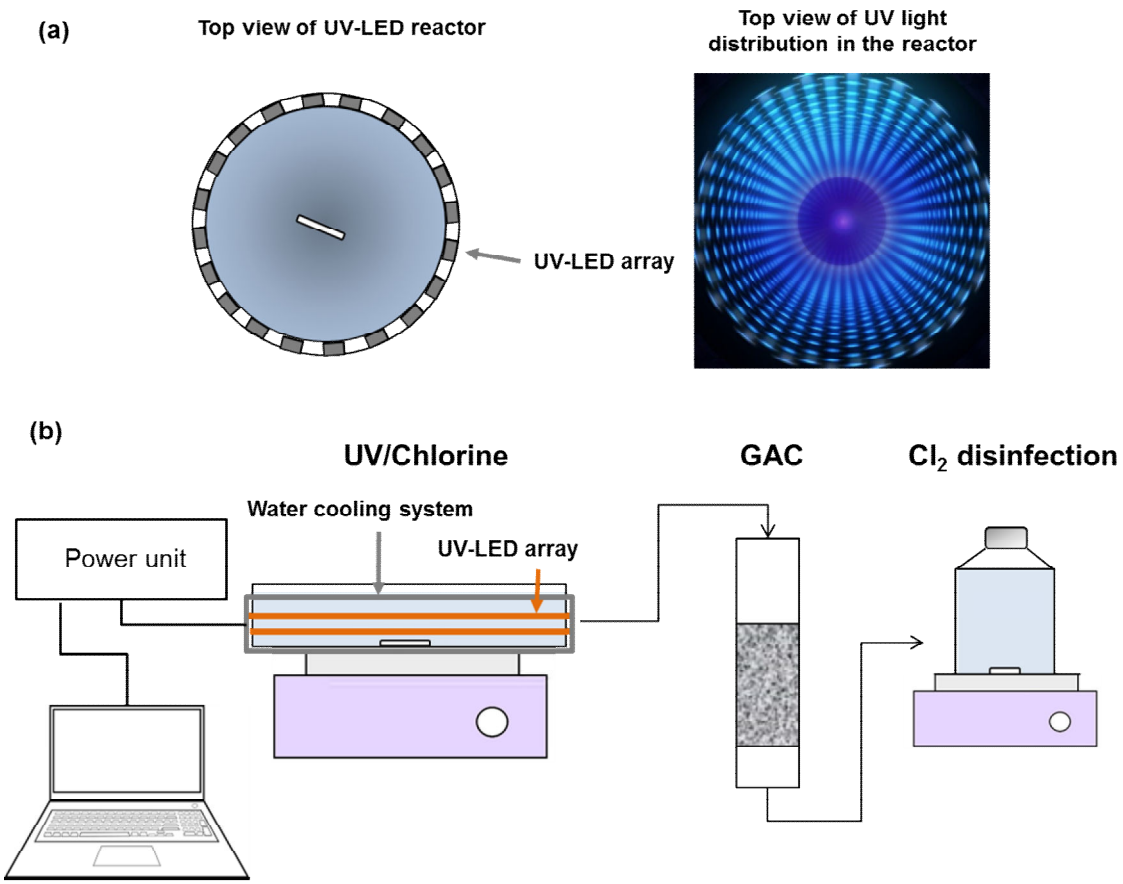

Figure 1. Diagram of top view of the UV-LED reactor and UV light distribution (a) and experimental set up (b).

Water samples were spiked so that the initial concentration of each pesticide (metaldehyde, carbetamide and mecoprop) was 300 ng/L. After collecting the samples from the different WTWs, samples were analysed for pesticide content and they were always found below 100 ng/L. Then the samples were topped up with pesticide to achieve 300 ng/L and measured again before the experiments to confirm the initial concentration. These pesticides are usually present in the sources under study. The pH was adjusted using sulphuric acid, and chlorine was added as sodium hypochlorite at the beginning of each experiment in one single dose or in sequential doses. The single chlorine concentrations tested were 1, 2, 4, and 6 mg/L at different pH values (Table 2). This concentration range has been reported as the values expected at a larger scale (Wang et al., 2015). Experiments with sequential chlorine doses (in lieu of one single chlorine addition) were carried out with 2 mg/L of chlorine added every 5 min. The sequential doses evaluated were 2 mg/L chlorine added three times or ten times. All experiments were carried out in duplicate with an experimental error below 7% in all cases.

In collimated beam tests where UV light is above the surface of the reactor, the light beams can be assumed to be parallel to each other and perpendicular to the irradiated surface. In this work, the light beams are in radial distribution, and merging in the centre of the reactor. Therefore, the reactor cannot be characterised by means of UV fluence (mJ/cm^2) as the irradiated volume is a non-uniform 3-dimensional space and UV dose derived from actinometry is not appropriate. The use of accumulated UV dose (accumulated mJ) would not be

appropriate either because of light distribution differences. Due to the complexity of the UV distribution in the reactor, and the fact that it is non-uniform, the experimental data have been expressed as a function of the Applied Optical Dose (AOD) (units J/L), defined as the optical energy applied to the system over time and relative to the reactor volume. For example, the optical power output for each UV-LED is 100 mW; hence the total optical power output for 40 UV-LEDs is 4.0 W. The volume is 3.15 L, so the AOD = [exposure time (s) * 4.0 W]/ 3.15 L. Experimental samples were taken at times 0, 1, 2, 5, 10, 15 and min, equivalent to an AOD of 76, 152, 381, 762, 1143, 2286 J/L, respectively. For the sequential chlorine dosage tests, chlorine was added after 0, 380 and 760 J/L for the three sequential doses; and after 0, 380, 760, 1140, 1520, 1900, 2280, 2660,3040, 3420 J/L for the ten chlorine sequential doses. The samples were filtered with 0.45 μm Millipore® filters with membranes made of mixed cellulose esters and quenched with sodium thiosulphate. Blank tests with chlorine only and UV photolysis were also carried out.

Table 2. Operational conditions used for the UV/Chlorine experiments.

Chlorine (mg/L)	**pH**						
	5.1	5.5	6	6.5	7	7.5	Natural pH*
1	✔			✔			✔
2	✔			✔			✔
3	✔			✔			✔
4	✔	✔	✔	✔	✔	✔	✔
6	✔			✔			✔

*Natural pH refers to the unmodified pH of the water samples (pH 7.9 for source A; pH 8 for source B; and pH 8.2 for source C)

2.4 Disinfection by-product formation, GAC adsorption and final disinfection tests.

The formation of DBPs before and after the UV/Chlorine process was monitored, using the optimum conditions (chlorine concentration and pH) for pesticide removal, based on the results from the experimental plan described in Section 2.3. Samples were quenched and analysed for THMs, HAAs and bromate. Samples were quenched with ammonium chloride prior to HAA analysis and with sodium sulphite for THM and bromate analysis.

In the UK, an oxidation process, such as ozonation or AOP, is typically followed by GAC adsorption prior to final disinfection. To understand how DBPs change after the UV/Chlorine process and subsequent treatment, the AOP treated water was passed through GAC adsorption columns and then disinfection was mimicked with an additional chlorine dose (Figure 1). AOP samples treated with 380 J/L were run through GAC treatment. The GAC column was filled with a ground GAC sample taken from one of the WTW. The sample was GAC Norit 1240 W with an iodine number of 975, 1100 m^2/g total surface area, 420 kg/m^3 apparent density, 0.6-0.7 effective size D_{10} and uniformity coefficient of 1.7 as provided by the supplier. The columns were set to achieve an empty bed contact time (EBCT) of 20 min, which was the contact time used on site. For the final disinfection simulation, 1 mg/L chlorine was added to the GAC treated samples, with a contact time of 30 min. These samples were compared to “untreated water” samples taken prior to AOP treatment.

2.5 Chemical analysis

The dissolved organic carbon (DOC) concentration was measured by a Shimadzu TOC-V analyser as non-purgeable organic carbon (NPOC). All samples were acidified in the instrument with 2 M HCl and purged with carbon-free air to remove inorganic carbon (carbonates and bicarbonates). The method used was calibrated to measure the DOC concentration in the 1-10 mg/L range. Chlorine was measured by using a portable Hach pocket colorimeter, with DPD reagent for analysis of free chlorine. Nitrate, phosphate, and chloride were analysed with ion chromatography. Ions were analysed by a Dionex®-ICS 1600 anion chromatograph with 2 mM sodium carbonate as the eluent. The injection volume was 50 μL. Flow was set to 1 mL/min and column temperature was kept constant at 35 °C. Bromide and bromate were analysed by an external laboratory by ion chromatography with an elution gradient with a limit of quantification of 0.35 µg/L. Pesticides were analysed using LC-MSMS using a method published elsewhere (Ramos et al., 2019). A Kinetex C18 column (5 μm 150 x 2.1 154 mm, Phenomenex, UK) thermostated at 60°C was used for chromatographic separation. The flow rate was 0.3 mL min^{-1} and the injection volume was 50 μL. The mobile phase consisted of ultrapure water with 0.1% acetic acid and methanol with 0.1% acetic acid. The elution started at 10% B and was linearly increased to 98% over 12 min, then maintained for 3 min before returning to the initial composition. The total time of analysis per sample was 18 min. The limits of quantification for metaldehyde, carbetamide and mecoprop were 0.01 µg/L, 0.01 µg/L and 0.05 µg/L, respectively.

267 THMs and HAAs were analysed in an Agilent GC-ECD 6890 with a capillary
268 column (Phenomenex 30m x 0.25 mm x 0.25 μm), following a modified extraction
269 of USEPA methods published elsewhere (Goslan, 2003; Bougeard et al., 2010).

3 Results and Discussion

3.1 Pesticide degradation

Higher pesticide removal was observed in source A, followed by sources C and B for a given pH value (Figures 2 and 3). Source A was taken from the outlet of UF membrane treatment, which resulted in higher UVT (92%) than sources B (79%) and C (87%), where samples were taken from rapid gravity filters (Section 2). Source A also had lower alkalinity and DOC (Table 1). It is known that carbonate and bicarbonate react with hydroxyl radicals, forming carbonate radicals, which are selective and less reactive than hydroxyl radicals (Busset et al., 2007). Sulphate concentrations were similar in the three sources (ca 115 mg/L).

The pH had a significant impact on the degradation rates for both metaldehyde and carbetamide (Figures 2 and 3). The conditions tested included a range of pH values between 5.1 and 8.2. The lower the pH, the higher the degradation rate of the pesticides. For pH 5.1, metaldehyde was degraded by 80%, 42% and 60% for sources A, B and C, respectively. At natural pH (pH 7.2-8.2), metaldehyde removal reached 18%, 16% and 7%, for sources A, B and C. In sources A and C, a plateau was achieved after 400 J/L, after which chlorine concentration was

consumed. For source B, chlorine degradation was slower arising from the physico-chemical properties of the water (lower UVT) and the plateau was achieved at an AOD of 1,200 J/L when the chlorine was consumed. Previous work from Jefferson et al. (2016) investigated the degradation of metaldehyde by the UV/H_2O_2 process in surface water and demonstrated that to achieve >95% metaldehyde removal a UV dose of 5,000 mJ/cm^2 in combination with a high H_2O_2 dose of (>200 mg/L) was required, showing the recalcitrant nature of this pesticide to treatment.

For carbetamide, the degradation rates were faster than for metaldehyde, which is in agreement with their second order kinetic rate constants (Autin, 2012). Complete degradation was achieved in source A for pH values lower than 7 and an AOD above 400 J/L. For higher pH, complete consumption of chlorine stopped the reaction. In source C carbetamide was completely removed at pH values below 6 and an AOD over 400 J/L. For higher pH values, carbetamide reached 94% removal at pH 6.5 and 62% at natural pH. In source B complete degradation was achieved at pH < 6, but in contrast to sources A and C, required a minimum AOD of 750 J/L. For higher pH, carbetamide removal varied from 82% (pH 6.5) to 45% (natural pH). The blanks (UV photolysis or chlorination) showed negligible degradation of metaldehyde and carbetamide. Mecoprop proved to be sensitive to photolysis at 285 nm, achieving complete degradation for AODs above 350 J/L dose, regardless of the water source. However, mecoprop degradation under the UV/Chlorine process was faster than with photolysis only, achieving complete degradation at an AOD of 100 J/L for all conditions, regardless of the water

source and pH (Figure S1). Ultrapure water tests containing pesticides only were also performed (data not shown), resulting in analogous trends in terms of pesticides removal, with mecoprop being removed the fastest and metaldehyde the slowest, and lower pH resulting in faster degradation in all cases.

For a given water source, the differences in pesticide removal were due to the chlorine chemistry in the water. When chlorine is dissolved into water, it reacts with water to form hypochlorous acid and hypochlorite ion which exist in equilibrium (eq. 1), and their relative speciation is dependent on pH (pK_a = 7.5 at 25 °C) (Feng et al., 2007).

(1) $HClO \rightleftharpoons ClO^- + H^+$

The effect of pH in the chlorine speciation is such that the predominant species at acidic pH is HOCl, and at basic pH the predominant species is the OCl^-. At pH 5.1 more than 99% of chlorine is as HOCl; while at pH 10 more than 99% of chlorine is as OCl^- (De Laat and Stefan, 2018). Both species can absorb photons and yield hydroxyl radicals. Hypochlorous acid forms hydroxyl and chlorine radicals when absorbing UV (eq 2). Hypochlorite ions absorb photons to form chlorine and atomic oxygen anion radicals (eq 3). Atomic oxygen anion radicals then react and form hydroxyl radicals (eq 4).

(2) $HClO + h\nu \rightarrow OH^\bullet + Cl^\bullet$

(3) $ClO^- + h\nu \rightarrow O^{-\bullet} + Cl^\bullet$

(4) $O^{-\bullet} + H_2O \rightarrow OH^\bullet + OH^-$

In addition, each species has different absorption spectra. Hypochlorous acid has an absorption peak at 248 nm with a molar absorption coefficient of 101 ± 2 M^{-1} cm^{-1}, and decreasing molar absorption coefficient up to approximately 350 nm. The absorption spectrum of hypochlorite has a higher peak at 292 nm (365 ± 8 M^{-1} cm^{-1} molar absorption coefficient) and a smaller absorption peak at 236 nm (ca 180 M^{-1} cm^{-1}) (Feng et al., 2007). In addition, although there is no information available information at 285 nm, at 254 nm the quantum yield for the formation of hydroxyl radicals at pH 10 has been found to be higher than at pH 5 (1.18 versus 0.79) (Wang et al., 2012). Therefore, it could be expected that operating the process at higher pH would encourage faster pesticide degradation where the emission wavelength is close to the maximum absorption peak of the hypochlorite, 285 nm. However, radical scavenging reactions are also dependent on the chlorine species. Hypochlorous acid reacts with hydroxyl radicals (eq 5) at a rate of 2 x 10^9 M^{-1} s^{-1} (Matthew and Anastasio, 2006) . Hypochlorite ions, however, react with hydroxyl radicals (eq 6) at a faster rate 8.8 x 10^9 M^{-1} s^{-1} (Buxton and Subhani, 1972). Therefore, at high pH the radical scavenging reaction is more predominant, explaining the faster degradation observed at lower pH.

(5) $OH^{\bullet} + HClO \rightarrow H_2O + ClO^{\bullet}$

(6) $OH^{\bullet} + ClO^{-} \rightarrow ClO^{\bullet} + OH^{-}$

Two chain-reactions have been proposed for the decomposition of HClO by hydroxyl radicals (eq 7 and 8) and by chlorine radicals (eq 9 and 10) (Oliver and Carey, 1977). Other secondary reactions include those between organic matter

and radicals. The results were also in agreement with this, since sources B and C had higher DOC content than source A, where pesticide degradation was faster.

(7) $OH^{\bullet} + RH \rightarrow \cdot R + H_2O$

(8) $\cdot R + HOCl \rightarrow RCl + OH^{\bullet}$

(9) $Cl^{\bullet} + RH \rightarrow R^{\bullet} + HCl$

(10) $R^{\bullet} + HOCl \rightarrow ROH + Cl^{\bullet}$

Overall, the results show that high UVT is needed for this process to be implemented at large scale. As an example, membrane filtration rather than rapid gravity filtration for treatment of Sources B and C could improve the level of pesticide degradation to that seen for source A. An effective DOC pre-treatment would also positively impact the micropollutant degradation rate. High UVT and DOC removal would extend the pH range at which the UV/Chlorine process could operate, reducing the use of chemicals to adjust pH or the chlorine dose, which would potentially impact DBP formation. In this regard alkalinity was another significant factor. For non-alkaline waters, the process would be able to remove the most persistent pesticides with small AODs (~0.40 J/L) and without high chemical costs for pH adjustment.

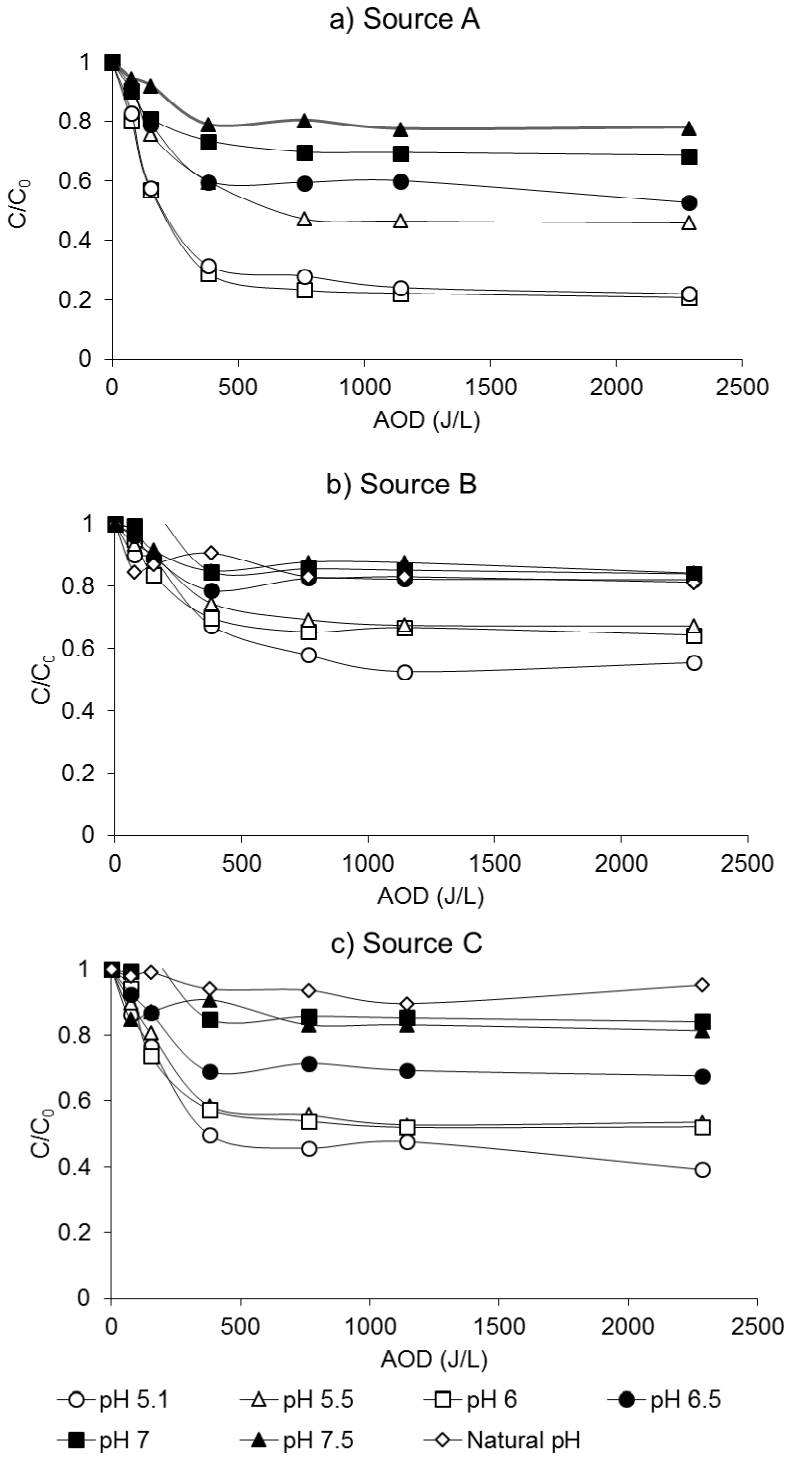

Figure 2. Metaldehyde degradation using a chlorine dose of 4 mg/L at different pH values for sources A, B and C. Natural pH refers to the unmodified pH of the water samples (pH 7.9 for source A; pH 8 for source B; and pH 8.2 for source C).

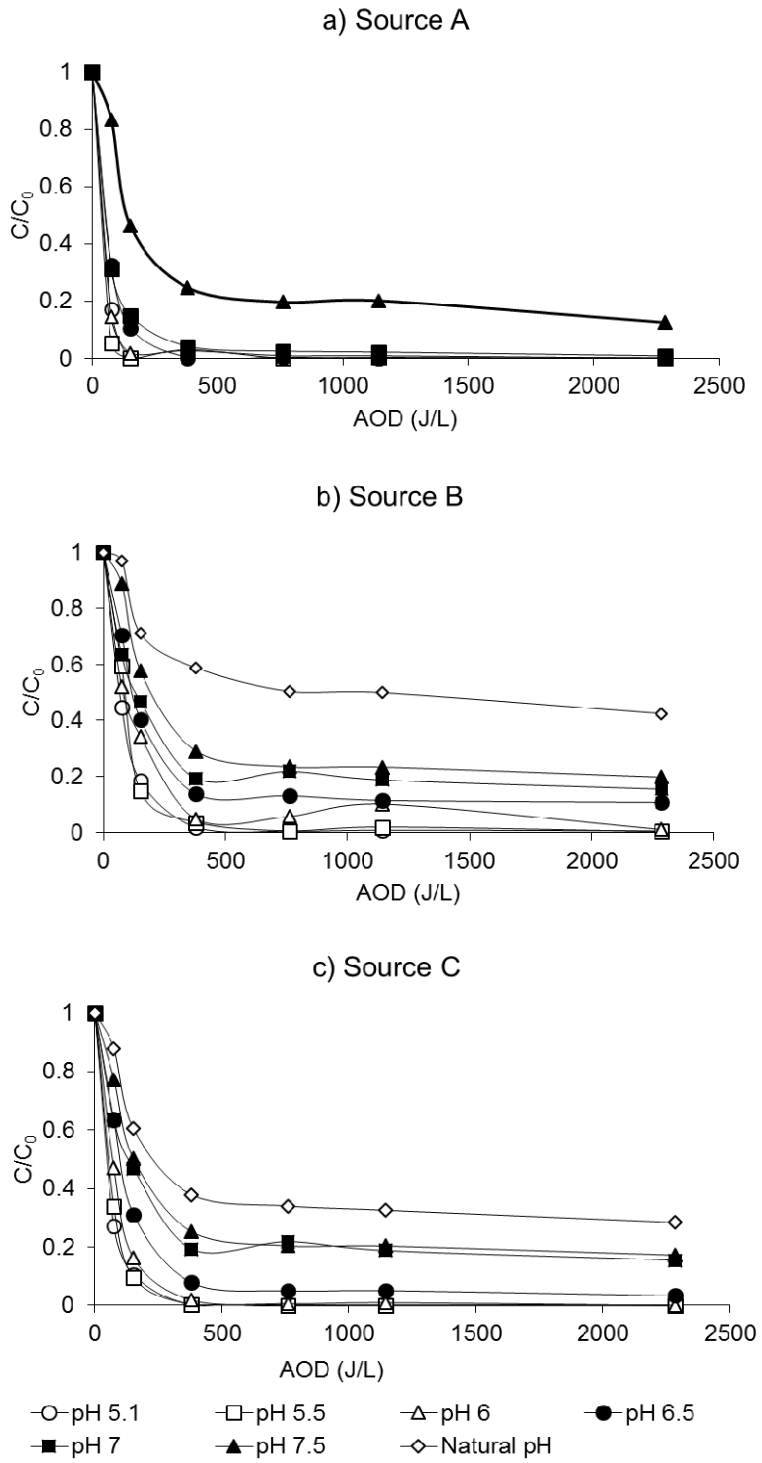

Figure 3. Carbetamide degradation using chlorine dose of 4 mg/L at different pH values for the sources A, B and C. Natural pH refers to the unmodified pH of the water samples (pH 7.9 for source A; pH 8 for source B; and pH 8.2 for source C).

Further analysis of the pesticides degradation was developed by calculating the pseudo-first order degradation rate constants (k') at various pH values and chlorine concentrations (1-6 mg/L) (Figure 4).

For both metaldehyde and carbetamide lowering the pH increased the degradation rate constant, k'. For metaldehyde, the increase in k' with chlorine concentration was less significant at pH 6.5 and at natural pH. Indeed, the value of k' was below 0.002 L/J at these pH values. At pH 5.1, where 99% of the chlorine was as HOCl, k' increased by a factor of seven from 0.0004 L/J for a chlorine dose of 1 mg/L to 0.0027 L/J for a chlorine dose of 6 mg/L. For a given pH, increasing the chlorine concentration beyond 4 mg/L did not significantly increase the k' value. This effect has been previously reported in the literature, where a target compound reaches a maximum degradation constant, and then the constant remains the same or decreases (Carra et al., 2014). The point at which this rate-limiting effect takes place is dependent on the water matrix and target compound (Carra et al., 2014). This effect acts in combination to the fact that an excess of chlorine promotes scavenging reactions (eq 7-10).

For carbetamide, k' was at least twice value seen for metaldehyde at equivalent pH and chlorine concentration. However, a rate-limiting effect was not observed for this pesticide, likely because of its higher reactivity towards hydroxyl radicals than metaldehyde. In this case, k' continued to increase at 6 mg/L of chlorine. Similarly to metaldehyde, at pH 6.5 and natural pH the k' values were closer for a given chlorine concentration, but increasing the fraction of hypochlorous acid

to 99% at pH 5.1 resulted in an increase in *k'* to double the values seen at natural pH. For mecoprop the degradation was too fast to obtain accurate kinetic data.

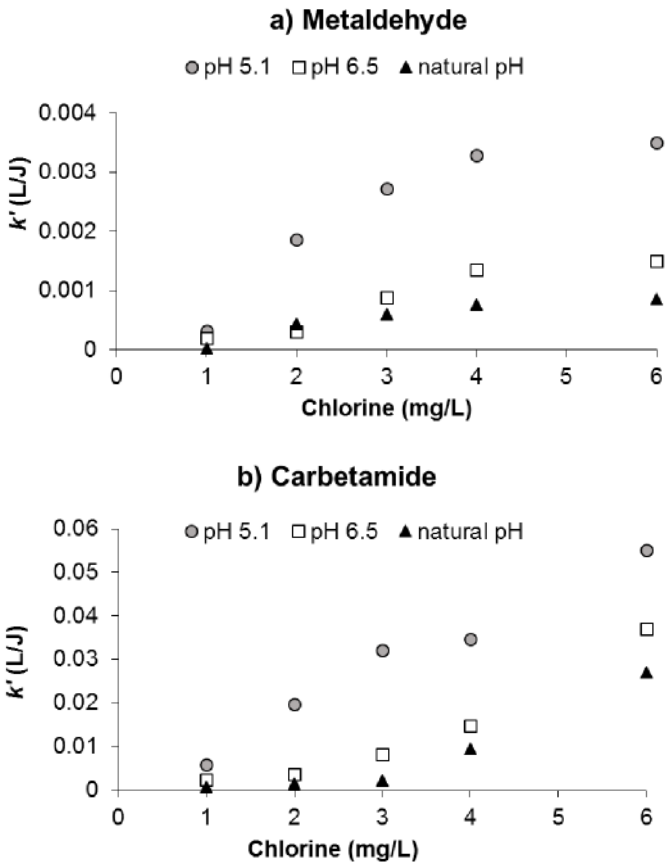

Figure 4. Metaldehyde and carbetamide pseudo first order degradation kinetic constants as a function of pH and chlorine for source A. Natural pH refers to the unmodified pH of the water samples (pH 7.9 for source A).

An analysis of variance (ANOVA) was run to determine whether there were any statistically significant differences between the chlorine concentration and the pH in response to the *k'* values for metaldehyde and carbetamide (Table S1). The results showed that the pH always had a significant impact over the degradation

constants at a 95% confidence interval, which was consistent with the experimental data. The significance of the chlorine concentration increased in sources B and C in comparison to A. This arose from the complexity of the water sources, with lower UVT and higher concentrations of scavenging ions and DOC in these water sources, which increased the effect of inefficient reactions and made the chlorine concentration a more significant factor.

The rate constants and the ANOVA calculations indicated that chlorine concentration gained significance, particularly when the water matrix was more complex or had low UVT. The addition of oxidants in AOPs is often a controlling factor for their application at larger scale. High chemical requirements can have a significant cost implication, and for drinking water in particular, minimising the use of chemicals is a driver for water utilities for reasons of sustainability, customer perception, taste and odour issues or by-product formation. Previous research has shown that optimising the oxidant dosage strategy may enhance the degradation kinetics of target pollutants by minimising inefficient reactions, such as radical-radical or oxidant-radical reactions. As a result, a continuous or sequential dose of the oxidant may result in improved pesticide removal versus an initial chemical addition at the beginning of the process (Carra et al., 2013). In this work, addition of chlorine at the beginning of the experiment was compared to its addition in smaller sequential doses (Section 2.3) (Figure 5). The experiments were carried out using source B samples, as the most challenging water, with higher alkalinity, nitrate concentration and lowest UVT. Metaldehyde was used as the target compound, as it was the most persistent to remove and

complete degradation would imply that carbetamide and mecoprop would be fully removed as well.

When an initial chlorine dose of 2 mg/L was added, metaldehyde removal was below 18%. Similar results were obtained when one single dose of 6 mg/L was added. However, if instead of adding 6 mg/L as one single dose we added it as a sequential dose of 2 mg/L added three times, metaldehyde's degradation increased to 40%. If the sequential dose continued, up to adding chlorine ten times, the degradation removal increased to almost 95%.

When chlorine is added in one single addition, the inefficient reaction between chlorine and hydroxyl radicals is promoted (eqs 4 and 5), but if chlorine is slowly dosed, those reactions are less favoured, and the radical-to-target compound reaction is promoted. Therefore, these results showed that optimising the dosage strategy is as important as optimising the chemical concentration. Nevertheless, a deeper study to understand dose strategies should be developed.

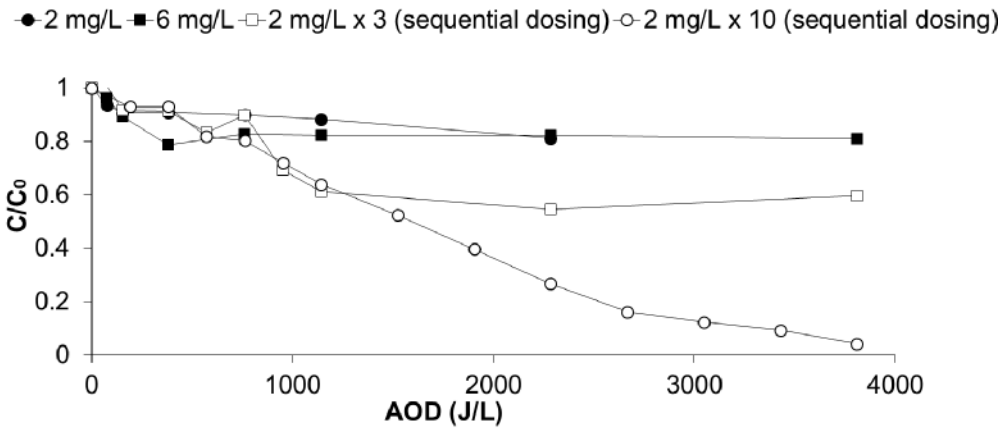

Figure 5. Metaldehyde degradation profiles with different chlorine dosing strategies (2 mg/L; 6 mg/L; 2 mg/L added 3 times; and 2 mg/L chlorine

added 10 times) in source B at pH 6.5. For the three sequential doses, chlorine was added at 0, 380 and 760 J/L; and for the ten sequential doses chlorine was added at 0, 380, 760, 1140, 1520, 1900, 2280, 2660,3040, 3420 J/L .

3.2 Disinfection by-product formation

DBPs are a consequence of the reaction between chlorine and organic matter, which would typically happen during final chlorine-based disinfection or at a pre-chlorination stage. Pesticides and other micropollutants are usually found at low concetrations in drinking water sources (µg/L). Thus, the main contributor to DBP formation is NOM. In addition, during chemical processes such as AOPs, organic matter is transformed, but the impact of this transformation on DBP formation potential is not yet fully understood.

The use of chlorine in combination with UV as an AOP raises the question of its impact on DBP formation. In this work, the formation of THMs and HAAs was monitored before and after the UV/Chlorine process, but also after GAC adsorption and final disinfection with chlorine. After AOP treatment a GAC adsorption stage may follow before final disinfection. This is to adsorb organic by-products, quench the residual chemical, and further remove organics (Collins and Bolton, 2016).

The results in this study showed an overall THM concentration increase when the pH was increased in the untreated samples (before UV/Chlorine treatment) for the three sources studied. For example, in source A there was an increase in

THM formation from 10 μg/L at pH 5.1 to 78 μg/L at pH 7.2 in the untreated samples (Figure 6). This is a well-known effect because of the importance of base-catalysed reaction steps (Diehl et al., 2000; Stevens et al., 1989).The UV/Chlorine process increased THM concentration between 20-30% at pH 5.1 and pH 6.5 in comparison to formation potential before AOP treatment, except for source C where THM concentration decreased after AOP treatment by 13%. However, at natural pH (pH 7.2-8.2) the UV/Chlorine process always decreased the THM concentration between 12 and 62% for the three sources. This can be explained by the efficiency of the process itself, which is lower at natural pH (Section 3.1), and is related to the speciation of chlorine at different pH. As a result, less oxidation was taking place in comparison to lower pH and the impact on DBP formation potential was lower. There is disagreement in the literature on the effect UV/Chlorine treatment has on THM formation. Wang et al. (2015) reported low THM formation at pH between 7.5-8.5 after treatment in a medium pressure reactor at pilot scale. Zhang et al. (2015) reported a reduction in THM formation after UV/Chlorine treatment in an annual reactor. However, an increase in THM formation during UV/Chlorine treatment has also been reported during humic acid degradation at 254 nm, 270 nm and 310 nm (Gao et al., 2016; Gao et al., 2019).

When the water samples were treated by GAC, the THM concentrations were always reduced to final concentrations between 3-16 μg/L for all sources, particularly at higher pH. This effect has been reported in the literature, where THM adsorption on GAC is favoured at higher pH values (Rasheed et al., 2016). The mass concentration adsorbed at natural pH for source A was 45 μg/L; and in

sources B and C, between 20-24 μg/L. The bromide concentration in source A was higher than in the other two sources (in the range 60-100 μg/L) (Table 1). As a result, bromoform and dibromochloromethane made up almost 60% of the total THM concentration for source A before GAC treatment, with 33-45% being adsorbed by the GAC; while in sources B and C it constituted less than 25% of the four THM species (species data not shown). The presence of bromide favours the formation of bromo-THM species, which adsorb better onto GAC than chloro-THM species through the formation of strong bonds between bromide and activated carbon (Babi et al., 2011).

After additional chlorine doses to simulate final disinfection conditions (post-disinfection samples in Figure 6), the THM levels increased again for all water sources, implying that organic precursors were still available after treatment with UV/Chlorine and GAC adsorption treatments. Nevertheless, the final THM values were always below 40 μg/L, regardless of pH and source, meeting current European and North American regulations.

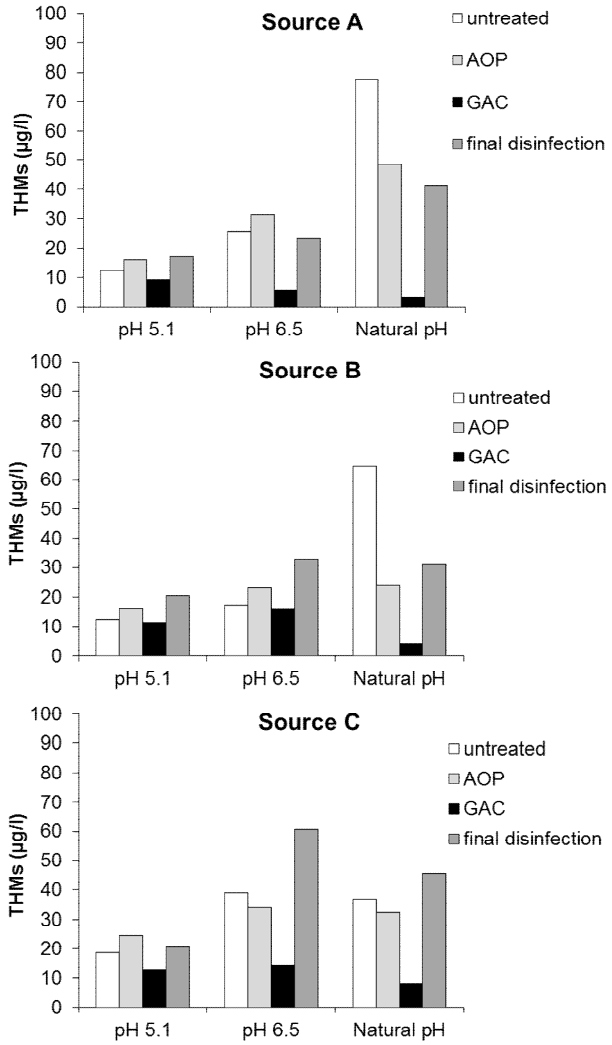

Figure 6. THM formation through UV/Chlorine treatment, GAC adsorption and final disinfection with chlorine. Natural pH refers to the unmodified pH of the water samples (pH 7.9 for source A; pH 8 for source B; and pH 8.2 for source C).

When looking at HAA formation, the concentrations were generally lower than THMs, ranging from 10 to 17 μg/L in the untreated samples (before UV/Chlorine treatment) (Figure 7). A strong pH effect was not observed, although slightly lower HAA concentrations were formed at higher pH. This trend was more significant for source B.

The UV/Chlorine process increased the formation of HAAs more strongly than THMs at pH 5.1 and pH 6.5, with post-AOP concentrations increasing by between 100-180% across the three sources. However, it is worth pointing out that these concentrations never exceeded 35 μg/L. As with THMs, contradicting results have been reported for HAAs. Zhou et al. (2016) reported an increase in HAAs after UV/Chlorine treatment under low pressure lamps; while Zhang et al. (2015) reported a decrease in HAA formation in an annual reactor with low pressure lamps.

When the samples were treated by GAC adsorption, the HAA concentrations were reduced, similarly to THMs. In source A, the HAA reduction after GAC was up to 80%, while for the other sources ranged between 45-60%. This also had to do with the speciation of the 9 HAAs analysed for. In source A, bromo-HAA species accounted for up to 25% of the total HAA9; while in sources B and C, they accounted for less than 10%, explaining the greater adsorption on GAC for water A as seen for the THMs.

After final disinfection, the HAA levels increased again, following the THM trend, but they were always below 18 μg/L, lower than THMs and compliant with current and expected HAA regulations.

Overall, the UV/Chlorine process did not increase THM formation significantly at acidic pH and, actually, at natural pH the THM concentrations were reduced. HAA formation however, was increased under acidic pH, but GAC treatment mitigates their formation, particularly at natural pH.

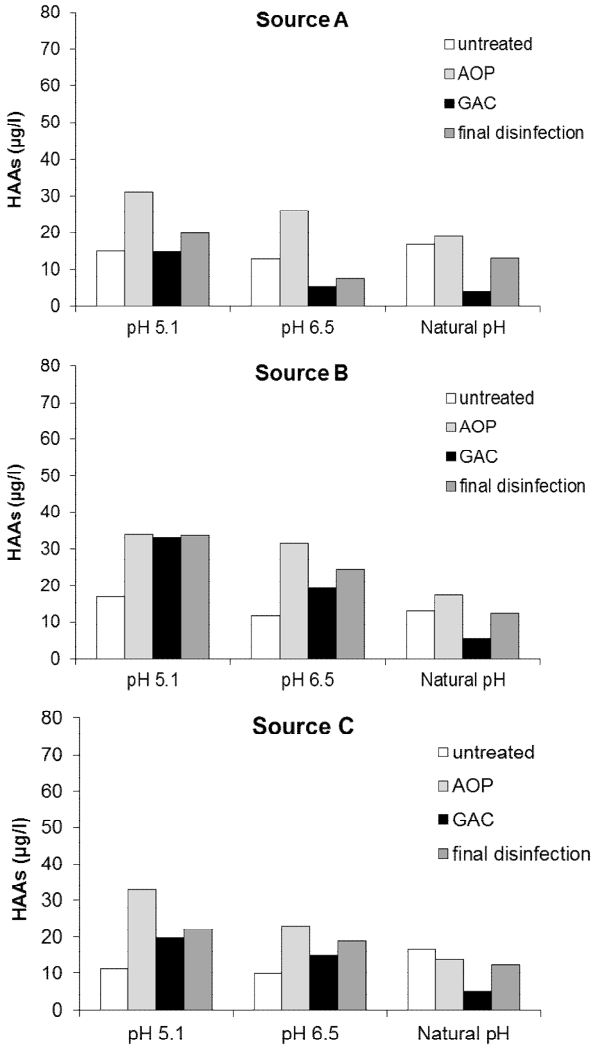

Figure 7. HAA formation through UV/Chlorine treatment, GAC adsorption and final disinfection with chlorine. Natural pH refers to the unmodified pH of the water samples (pH 7.9 for source A; pH 8 for source B; and pH 8.2 for source C).

The formation of bromate during the UV/Chlorine process, when using low and medium pressure lamps, has been reported (Fang et al., 2017a). However, as far as the authors are aware, bromate formation has never been studied at the specific wavelength of this work (285 nm). Bromate is an inorganic DBP,

regulated at 10 μg/L in the EU and US, which can be formed under certain conditions when bromide is present in water. Bromide is oxidised to hypobromous acid or hypobromite (eqs 11, 12), depending on pH, and then to bromate by hydroxyl radicals (eq 13). However, it is a complex process as chlorine radicals and other radicals are also suspected to be involved in bromate formation (eq 11-13) (Fang et al., 2017b).

(11) $HClO + Br^- \rightarrow HBrO + Cl^-$

(12) $ClO^- + Br^- \rightarrow BrO^- + Cl^-$

(13) $HBrO/BrO^- + OH^\bullet \rightarrow BrO_3^-$

Source A was used for the experimental work since it had the highest bromide concentration. Bromate concentration was monitored before and after the AOP, but also after GAC adsorption at different pH values (Figure 8). The untreated water already contained a low concentration of bromate (<4 μg/L). After the UV/Chlorine process, bromate concentration slightly increased at pH 5.1 and 6.5, with a bromate value of 4.7 μg/L. At natural pH the bromate concentration increased to 11 μg/L. These results agree with those reported by Fang et al. (2017a) where higher pH values resulted in increased bromate formation under low and medium pressure lamps. However, Wang et al. (2015) found that bromate formation increased more at lower pH under medium pressure lamps. When the water was treated by GAC, bromate was reduced to values below 3 μg/L. This agrees with other work that has established that activated carbon is effective for the removal of bromate (Bao et al., 1999; Zhang et al., 2015). However, the capacity and breakthrough of bromate with GAC needs to be

determined to understand the long-term feasibility of applying adsorbents for this role.

Other studies have shown that operational conditions and background water quality are important factors that influence micropollutant control, and therefore will be site specific. This is an important aspect to bear in mind when applying the UV/Chlorine process, as the chlorine concentration and applied optical dose would need to be optimised for the removal of the target pollutants, but also tailored to minimise DBP formation.

The results show for the first time the impact of process conditions on the DBPs that form with the UV/Chlorine process using LEDs for real water samples. The results show that as long as GAC adsorption is placed after the process, all DBPs studied can be controlled. However, if DBPs have to be controlled only with the UV/Chlorine process, a deeper study should be carried out to find the optimum combination of chlorine and applied optical dose which would allow for the removal of target compounds while minimising DBP formation, including the water quality of the untreated water.

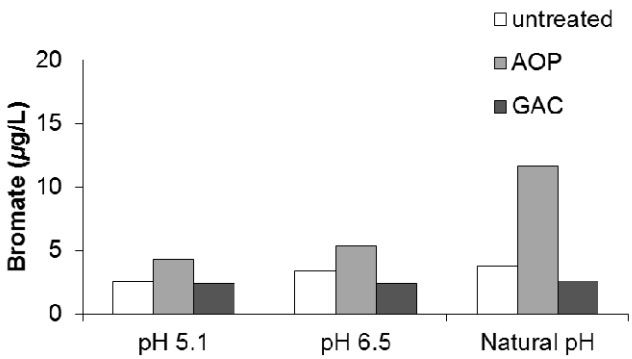

Figure 8. Bromate formation after the UV/Chlorine process and GAC adsorption in source A. Natural pH refers to the unmodified pH of the sample, pH 7.9.

4 Conclusions

This work has shown the feasibility of using the UV/Chlorine process with UV-LEDs for the removal of pesticides in drinking water. The results suggest a compromise is needed between pH, chlorine concentration and the chlorine dosing strategy to remove pesticides efficiently, but also to minimise DBP formation. Effective pre-treatment is needed to ensure high UVT and low DOC conditions. This allows the process to be carried out without the need to adjust pH. In addition, lower chlorine concentrations can be used while using low AODs. Further work should be developed to understand the importance of the chlorine dose strategy.

This is the first time that a study of THM, HAA and bromate formation in complex water matrices with an LED-UV/Chlorine system and the mitigating impact of subsequent GAC treatment has been reported. Overall, the UV/Chlorine process did not significantly increase THM or HAA formation at natural pH at the studied wavelength. At acidic pH however, THM and HAA formation increased. In all cases, results showed that GAC treatment mitigated DBP formation, particularly at higher pH values. Future research should be directed at understanding the synergies between the combination of UV/Chlorine and GAC for DBP minimisation. However, the use of the UV/Chlorine process without GAC treatment, requires case-by-case consideration to determine the optimum

combination of chlorine and AOD which would allow for the removal of target compounds while minimising DBP formation, including the water quality of the untreated water.

ACKNOWLEDGEMENTS

This work was supported by Anglian Water and Typhon Treatment Systems.

REFERENCES

Autin, O., 2012. Micropollutant removal by Advanced Oxidation Processes. PhD thesis, Cranfield University.

Babi, K.G., Koumenidis, K.M., Makri, C.A., Nikolau, A.., Lekkas, T.D., 2011. Adsorption capacity of GAC pilot filter-adsorber and postfilter- adsorber for individual THMs from drinking water, Athens. Glob. NEST JournalGlobal NEST Int. J. 13, 50–58. https://doi.org/10.30955/gnj.000698

Bao, M.L., Griffini, O., Santianni, D., Barbieri, K., Burrini, D., Pantani, F., 1999. Removal of bromate ion from water using granular activated carbon. Water Res. 33, 2959–2970. https://doi.org/10.1016/S0043-1354(99)00015-9

Beck, S.E., 2018. UV LED Disinfection 101. IUVA News 20(1), 4-9 .

Bougeard, C.M.M., Goslan, E.H., Jefferson, B., Parsons, S.A., 2010. Comparison of the disinfection by-product formation potential of treated waters exposed to chlorine and monochloramine. Water Res. 44, 729–740. https://doi.org/10.1016/j.watres.2009.10.008

Busset, C., Mazellier, P., Sarakha, M., De Laat, J., 2007. Photochemical generation of carbonate radicals and their reactivity with phenol. J. Photochem. Photobiol. A Chem. 185, 127–132. https://doi.org/10.1016/j.jphotochem.2006.04.045

Buxton, G. V., Subhani, M.S., 1972. Radiation chemistry and photochemistry of oxychlorine ions. Part 3.-Photodecomposition of aqueous solutions of

chlorite ions. J. Chem. Soc. Faraday Trans. 1 Phys. Chem. Condens. Phases 68, 970–977. https://doi.org/10.1039/F19726800970

Carra, I., Casas López, J.L., Santos-Juanes, L., Malato, S., Sánchez Pérez, J.A., 2013. Iron dosage as a strategy to operate the photo-Fenton process at initial neutral pH. Chem. Eng. J. 224, 67–74. https://doi.org/10.1016/j.cej.2012.09.065

Carra, I., García Sánchez, J.L., Casas López, J.L., Malato, S., Sánchez Pérez, J.A., 2014. Phenomenological study and application of the combined influence of iron concentration and irradiance on the photo-Fenton process to remove micropollutants. Sci. Total Environ. 478, 123–132. https://doi.org/10.1016/j.scitotenv.2014.01.066

Collins, J., Bolton, J.R., 2016. Advanced Oxidation Handbook, ISBN 9781583219, American Water Works Association.

De Laat, J., Stefan, M., 2018. Chapter 9: UV/Chlorine process, in: Advanced Oxidation Processes for Water Treatment: Fundamentals and Applications. pp. 383–428.

Diehl, A.C., Speitel, G.E., Symons, J.M., Krasner, S.W., Hwang, C.J., Barrett, S.E., 2000. DBP formation during chloramination. J. / Am. Water Work. Assoc. 92, 76–90.

DWI, 2017. Summary of the Chief Inspector's report for drinking water in England, UK Drinking Water Inspectorate.

Fang, J., Zhao, Q., Fan, C., Shang, C., Fu, Y., Zhang, X., 2017a. Bromate

formation from the oxidation of bromide in the UV/chlorine process with low pressure and medium pressure UV lamps. Chemosphere. https://doi.org/10.1016/j.chemosphere.2017.05.136

Fang, J., Zhao, Q., Fan, C., Shang, C., Fu, Y., Zhang, X., 2017b. Bromate formation from the oxidation of bromide in the UV/chlorine process with low pressure and medium pressure UV lamps. Chemosphere 183, 582–588. https://doi.org/https://doi.org/10.1016/j.chemosphere.2017.05.136

Feng, Y., Smith, D.W., Bolton, J.R., 2007. Photolysis of aqueous free chlorine species (HOCl and OCl –) with 254 nm ultraviolet light. J. Environ. Eng. Sci. 6, 277–284. https://doi.org/10.1139/s06-052

Gao, Z., Lin, Y., Xu, B., Xia, Y., Hu, C., Zhang, T., Cao, T., Chu, W., Gao, N., 2019. Effect of UV wavelength on humic acid degradation and disinfection by-product formation during the UV / chlorine process. Water Res. 154, 199–209. https://doi.org/10.1016/j.watres.2019.02.004

Goldstein, S., Aschengrau, D., Diamant, Y., Rabani, J., 2007. Photolysis of Aqueous H2O2: Quantum Yield and Applications for Polychromatic UV Actinometry in Photoreactors. Environ. Sci. Technol. 41, 7486–7490. https://doi.org/10.1021/es071379t

Goslan, E. H., Natural organic matter character and reactivity: assessing seasonal variation in a moorland water, 2003. PhD Thesis, Cranfield University

Jefferson, B., Jarvis, P., Bhagianathan, G.K., Smith, H., Autin, O., Goslan, E.H.,

MacAdam, J., Carra, I., 2016. Effect of elevated UV dose and alkalinity on metaldehyde removal and THM formation with UV/TiO2 and UV/H2O2. Chem. Eng. J. 288, 359–367. https://doi.org/10.1016/j.cej.2015.11.071

Jin, J., El-Din, M.G., Bolton, J.R., 2011. Assessment of the UV/Chlorine process as an advanced oxidation process. Water Res. 45, 1890–1896. https://doi.org/10.1016/j.watres.2010.12.008

Macnulty, P., 2019. A method, system and apparatus for treatment of fluids. GB2567342A. Retrieved from https://patents.google.com/patent/GB2567342A/en

Matthew, B.M., Anastasio, C., 2006. A chemical probe technique for the determination of reactive halogen species in aqueous solution: Part 1 - Bromide solutions. Atmos. Chem. Phys. 6, 2423–2437. https://doi.org/10.5194/acp-6-2423-2006

Miklos, D.B., Remy, C., Jekel, M., Linden, K.G., Drewes, J.E., Hübner, U., 2018. Evaluation of advanced oxidation processes for water and wastewater treatment – A critical review. Water Res. 139, 118–131. https://doi.org/10.1016/j.watres.2018.03.042

Muramoto, Y., Kimura, M., Nouda, S., 2015. Development and future of ultraviolet light-emitting diodes UV-LED will replace UV lamp. 2015 IEEE Summer Top. Meet. Ser. SUM, 13–14. https://doi.org/10.1109/PHOSST.2015.7248169

Oliver, B.G., Carey, J.H., 1977. Photochemical Production of Chlorinated Organics in Aqueous Solutions Containing Chlorine. Environ. Sci. Technol.

11, 893–895. https://doi.org/10.1021/es60132a003

Ortega, K., 2018. WRD GRIP UV/Cl2 AOP for Indirect Potable Reuse. IUVA news 20, 3–10.

Oturan, M.A., Aaron, J.J., 2014. Advanced oxidation processes in water/wastewater treatment: Principles and applications. A review. Crit. Rev. Environ. Sci. Technol. 2577–2641. https://doi.org/10.1080/10643389.2013.829765

Ramos, A. M., Whelan M. J., Cosgrove S., Villa, R., Jefferson, B. Campo. P., Jarvis, P., Guyme, I., 2019. A multi-component method to determine pesticides in surface water by liquid-chromatography tandem quadrupole mass spectrometry. Water Environ. J. 31(3). 380-387. doi:10.1111/wej.12254.

Rasheed, S., Campos, L.C., Kim, J.K., Zhou, Q., Hashmi, I., 2016. Optimization of total trihalomethanes' (TTHMs) and their precursors' removal by granulated activated carbon (GAC) and sand dual media by response surface methodology (RSM). Water Sci. Technol. Water Supply 16, 783–793. https://doi.org/10.2166/ws.2015.175

Reckhow, D.A., Linden, K.G., Kim, J., Shemer, H., Makdissy, G., 2010. Effect of UV treatment on DBP formation. J. / Am. Water Work. Assoc. 102, 100–113.

Remucal, C.K., Manley, D., 2016. Emerging investigators series: The efficacy of chlorine photolysis as an advanced oxidation process for drinking water treatment. Environ. Sci. Water Res. Technol. 2, 565–579.

https://doi.org/10.1039/c6ew00029k

Stevens, A. A., Moore, L.A., Miltner, R.J., 1989. Formation and control of non-trihalomethane disinfection by-products. J. Am. Water Work. Assoc. 81, 54–60.

Taghipour, K., Fariborz and Oguma, 2019. UV LED System Design, Operation and Application for Water Treatment. UV Solut. Mag. Quarter 1. https://uvsolutionsmag/articles/2019/ev-led-system-design-operation-and-application-for-water-treatment/.

Wang, C., Moore, N., Bircher, K., Andrews, S., Hofmann, R., 2019. Full-scale comparison of UV/H2O2 and UV/Cl2 advanced oxidation: The degradation of micropollutant surrogates and the formation of disinfection byproducts. Water Res. 161, 448–458. https://doi.org/10.1016/j.watres.2019.06.033

Wang, D., Bolton, J.R., Hofmann, R., 2012. Medium pressure UV combined with chlorine advanced oxidation for trichloroethylene destruction in a model water. Water Research 46(15), 4677-4686.

Wang, D., Bolton, J.R., Andrews, S.A., Hofmann, R., 2015. Formation of disinfection by-products in the ultraviolet/chlorine advanced oxidation process. Sci. Total Environ. 518–519, 49-57. https://doi.org/10.1016/j.scitotenv.2015.02.094

Yang, X., Sun, J., Fu, W., Shang, C., Li, Y., Chen, Y., Gan, W., Fang, J., 2016. PPCP degradation by UV/chlorine treatment and its impact on DBP formation potential in real waters. Water Res. 98, 309–318.

https://doi.org/10.1016/j.watres.2016.04.011

Zhang, X., Li, W., Blatchley, E.R., Wang, X., Ren, P., 2015. UV/chlorine process for ammonia removal and disinfection by-product reduction: Comparison with chlorination. Water Res. 68, 804–811. https://doi.org/10.1016/j.watres.2014.10.044

Zhou, S., Xia, Y., Li, T., Yao, T., Shi, Z., Zhu, S., 2016. Degradation of carbamazepine by UV / chlorine advanced oxidation process and formation of disinfection by-products 23, 16448–16455. https://doi.org/10.1007/s11356-016-6823-x

Supplementary Information

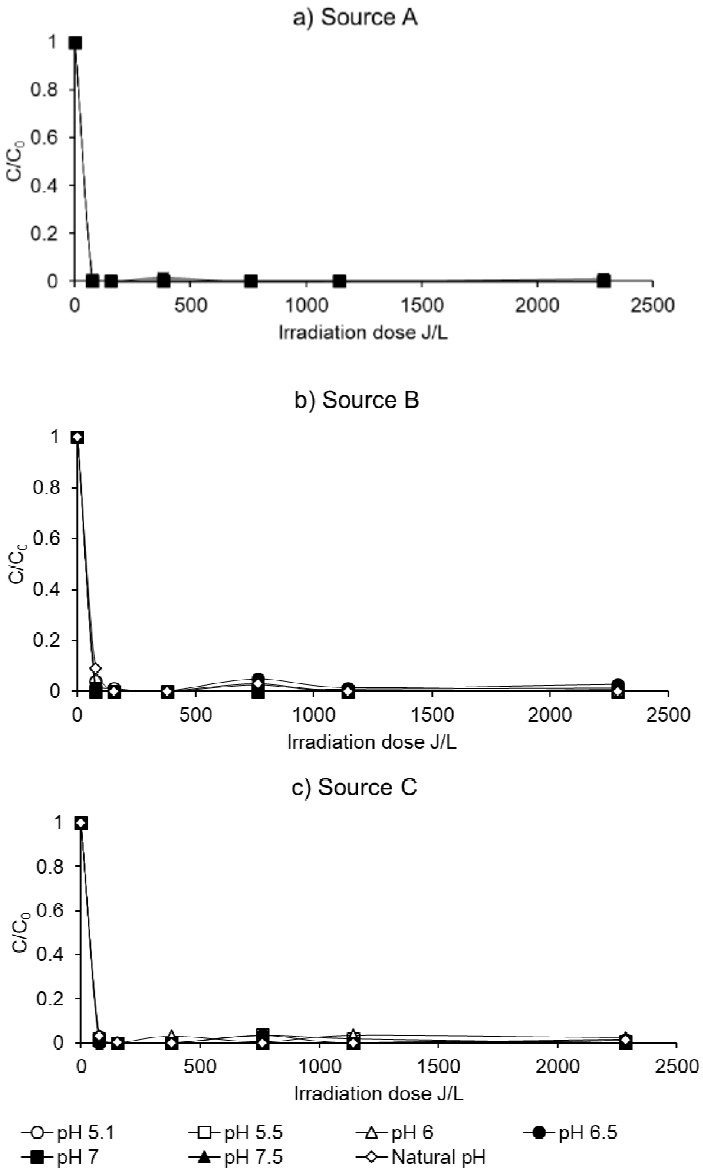

Figure S1. Mecoprop degradation using a chlorine dose of 4 mg/L at different pH values for sources A, B and C. Natural pH refers to the unmodified pH of the water samples (pH 7.9 for source A; pH 8 for source B; and pH 8.2 for source C).

Table S1. ANOVA results for the different sources and *k'* in L/J.

ANOVA Parameters	Source A		Source B		Source C	
	$k_{metaldehyde}$	$k_{carbetamide}$	$k_{metaldehyde}$	$k_{carbetamide}$	$k_{metaldehyde}$	$k_{carbetamide}$
p-Value for chlorine	0.068	0.051	<u>0.018</u>	0.057	<u>0.024</u>	0.057
p-Value for pH	<u>0.014</u>	<u>0.007</u>	<u>0.030</u>	<u>0.039</u>	<u>0.009</u>	<u>0.006</u>
R^2	0.782	0.807	0.919	0.803	0.931	0.830

p-values underlined correspond to values≤0.05

Figure Captions

Figure 1. Diagram of top view of the UV-LED reactor and UV light distribution (a) and experimental set up (b).

Figure 2. Metaldehyde degradation using a chlorine dose of 4 mg/L at different pH values for sources A, B and C. Natural pH refers to the unmodified pH of the water samples (pH 7.9 for source A; pH 8 for source B; and pH 8.2 for source C).

Figure 3. Carbetamide degradation using chlorine dose of 4 mg/L at different pH values for the sources A, B and C. Natural pH refers to the unmodified pH of the water samples (pH 7.9 for source A; pH 8 for source B; and pH 8.2 for source C).

Figure 4. Metaldehyde and carbetamide pseudo first order degradation kinetic constants as a function of pH and chlorine for source A. Natural pH refers to the unmodified pH of the water samples (pH 7.9 for source A).

Figure 5. Metaldehyde degradation profiles with different chlorine dosing strategies (2 mg/L; 6 mg/L; 2 mg/L added 3 times; and 2 mg/L chlorine added 10 times) in source B at pH 6.5.

Figure 6. THM formation through UV/Chlorine treatment, GAC adsorption and final disinfection with chlorine. Natural pH refers to the unmodified pH of the water samples (pH 7.9 for source A; pH 8 for source B; and pH 8.2 for source C).

Figure 7. HAA formation through UV/Chlorine treatment, GAC adsorption and final disinfection with chlorine. Natural pH refers to the unmodified pH of the water samples (pH 7.9 for source A; pH 8 for source B; and pH 8.2 for source C).

Figure 8. Bromate formation after the UV/Chlorine process and GAC adsorption in source A. Natural pH refers to the unmodified pH of the sample, pH 7.9.

Figure S1. Mecoprop degradation using a chlorine dose of 4 mg/L at different pH values for sources A, B and C. Natural pH refers to the unmodified pH of the water samples (pH 7.9 for source A; pH 8 for source B; and pH 8.2 for source C).